# A Semi-Empirical Method for Representing Domestic Refrigerator/Freezer Compressor Calorimeter Test Data

**Dagmar I. Jähnig**
*Associate Member ASHRAE*

**Douglas T. Reindl, Ph.D., P.E.**
*Member ASHRAE*

**Sanford A. Klein, Ph.D.**
*Fellow ASHRAE*

## ABSTRACT

*Mass flow rate and power calorimeter test data for domestic refrigerator/freezer fully hermetic compressors have been collected on compressors from three manufacturers. The calorimeter test data were taken by 10 different organizations. These test data are commonly correlated with 10-coefficient polynomials (using the method presented in* ARI Standard 540-91*) as a function of the saturated evaporator and condenser temperatures. In general, these polynomial representations accurately represent the experimental data but do not necessarily provide reliable interpolations or extrapolations for conditions not represented in the compressor calorimeter tests.*

*A semi-empirical model to represent compressor performance has been investigated. The model is based on the concept of volumetric efficiency and assumes a polytropic compression process. The model has five parameters that must be determined by fitting experimental data. Four or more measurements of refrigerant flow rate and compressor power were found to be sufficient to determine the model parameters, thereby allowing the generation of accurate compressor maps with the model. The model has been found to extrapolate within 5% error with condensing and evaporating temperatures that extend beyond the measured data by 10°C (18°F). A small set of available data for suction temperatures other than 32.2°C (90°F) were investigated. The results indicate that the model can accurately model the effect of changes in the suction temperature.*

## INTRODUCTION

Domestic refrigerators and freezers have become increasingly more energy efficient over the past decade. These performance improvements have been driven, in part, by federal standards (AHAM 1993) that have mandated higher minimum refrigerator/freezer product energy efficiency levels. The easy methods for improving energy efficiency of refrigerator/freezer products, e.g., improved seals on doors and better insulation, have already been exploited. Further product efficiency improvements will likely require a better integration and application of compressors (the single largest energy consumer in a refrigerator/freezer) into products.

The single point condition currently used for rating refrigerator/freezer compressors are an evaporating temperature of –23.3°C (–10°F) and a condensing temperature of 54.4°C (130°F) in a 32.2°C (90°F) environment. This rating point is commonly used in the industry but is not explicitly defined in any standard. This condensing temperature may have been appropriate years ago when refrigerators/freezers used natural convection condensers; however, most modern refrigerator/freezer appliances employ forced air condensers that lead to saturated condensing temperatures significantly lower than 54.4°C (130°F). In addition, some compressors are used solely in refrigeration cycles for which the saturated evaporating temperature is much higher than –23.3°C (–10°F); consequently, the –23.3°C (–10°F) test point is not useful for applying compressors in these products. A further complication is that most manufacturers of small hermetic compressors provide test data only at 32.2°C (90°F) suction temperature although the suction temperature during typical operation of a refrigerator/freezer may be much lower. It is necessary to accurately know the refrigerant mass flow rate and power of a compressor over a range of evaporator, condenser, and ambient temperatures in order to design efficient appliances. Since it is expensive and time consuming

**Dagmar I. Jähnig** is a research engineer in the HVAC&R Center and **Douglas T. Reindl** and **Sanford A. Klein** are professors at the University of Wisconsin, Madison.

*the American Society of Civil Engineers* 99(P01): 89-103.

Kavanaugh, S.P., and K. Rafferty. 1997. *Ground-source heat pumps. Design of geothermal systems for commercial and institutional buildings*. Atlanta: American Society of Heating, Refrigerating and Air-Conditioning Engineers, Inc.

Kavanaugh, S.P. 1998. A design method for hybrid ground source heat pumps. *ASHRAE Transactions* 104(2): 691-698.

Kishore, V.V.N., and V. Joshi. 1984. A practical collector efficiency equation for nonconvecting solar ponds. *Solar Energy* 33(5): 391-395.

SEL. 1997. 1997. *TRNSYS, A Transient Systems Simulation Program, User's Manual, Version 14.2*. Solar Energy Laboratory, University of Wisconsin-Madison.

McAdams, W.H. 1954. *Heat transmission,* 3d ed. McGraw-Hill Book Company.

Newell, T.A. 1984. Solar ponds—Alternate energy systems. *Military Engineer, Journal of the Society of American Military Engineers,* March-April, 492: 110-113.

Ogershok, D., and D. Phillips. 1999. *National construction estimator,* 47th ed. Carlsbad: Craftsman Book Company.

Pezent, M.C., and S.P. Kavanaugh. 1990. Development and verification of a thermal model of lakes used with water source heat pumps. *ASHRAE Transactions* 96(1): 574-582.

Raphael, J.M. 1962. Prediction of temperatures in rivers. *Journal of the Power Division, Proceedings of the American Society of Civil Engineers,* July, 88(P02): 157-181.

Rubin, H., B.A. Benedict, and S. Bachu. 1984. Modeling the performance of a solar pond as a source of thermal energy. *Solar Energy* 32(6): 771-778.

Schoen, F. 1999. Personal communication.

Spencer, J.W. 1971. Fourier series representation of the position of the sun. *Search* 2(5).

Spitler, J.D., C. Marshall, R. Delahoussaye, and M. Manicham. 1996. *Users Guide of GLHEPRO*. Stillwater, Okla.: School of Mechanical and Aerospace Engineering, Oklahoma State University.

Srinivasan, J., and A. Guha. 1987. The effect of reflectivity on the performance of a solar pond. *Solar Energy* 39(4): 361-367.

Wadivkar, O. 1997. *An experimental and numerical study of the thermal properties of a bridge deck de-icing system.* Unpublished master's thesis, Oklahoma State University, Stillwater.

Yavuzturk, C., and J.D. Spitler. 1999. A short time step response factor model for vertical ground-loop heat exchangers. *ASHRAE Transactions*, 105(2): 475-485.

Yavuzturk, C., J. D. Spitler, and S. J. Rees. 1999. A transient two-dimensional finite volume model for the simulation of vertical U-tube ground heat exchangers. *ASHRAE Transactions* 105(2): 527-540.

Yavuzturk, C. 1999. Modeling of vertical ground loop heat exchangers for ground source heat pump systems. Ph.D. thesis, School of Mechanical and Aerospace Engineering, Oklahoma State University.

to experimentally determine these data, developing a method to reliably interpolate and/or extrapolate experimental compressor data can substantially reduce this cost.

## DATA

Twenty-one sets of calorimeter test data for fully hermetic reciprocating refrigerator/freezer compressors have been collected on compressors from three manufacturers using R-134a or R-12 as the refrigerant. The calorimeter test data were taken by ten different organizations. All of these data were taken at an ambient, compressor suction, and liquid line temperature of 32.2°C (90°F). The compressors were tested at nine to seventeen different operating conditions (different saturated evaporating and condensing temperatures). The condensing temperatures ranged from 32.2°C (90°F) to 60°C (140°F) and the evaporating temperature ranged from –28.9°C (–20°F) to –12.2°C (10°F). For each evaporating and condensing condition, experimental values of the electrical power input and refrigerant mass flow rate (or refrigeration capacity) are given. The temperature of the refrigerant measured at the compressor discharge and/or the temperature on the dome of the compressor shell were also provided by14 of the data sets. The airflow rate past the shell for these tests was either 11.5 m/s (3.5 fps), 14.3 m/s (4.3 fps), or was not reported. Table 1 shows the codes that were used to identify the different data sets (uppercase letters show different manufacturers, lowercase letters different testing organizations). Two additional sets of data were obtained for ambient temperatures of 14.3°C (57.7°F), 16°C (61°F), 38.5°C (101°F), and 43.3°C (110°F).

## BIVARIATE POLYNOMIAL CURVE FIT

A method for representing compressor test data is described in ARI Standard 540 (ARI 1991). There is a revision of the standard from 1999, but the base equations and the computer program that is provided with it have not changed. The standard specifically excludes compressors used for domestic refrigerator/freezer appliances; nevertheless, the

**TABLE 1**
**Average Relative Errors (%) Obtained When Using All Data Points to Perform a Least Squares Curve Fit for the 10-Parameter Polynomial and the New 5-Parameter Model**

| | | 10-Coefficient Polynomial | | New 5-Parameter Model | |
|---|---|---|---|---|---|
| Data Set Code | Number of Data Points | Mass Flow Rate | Power | Mass Flow Rate | Power |
| A1a | 16 | 0.9 | 0.7 | 5.2 | 1.4 |
| A1b | 14 | 0.2 | 0.2 | 0.8 | 0.9 |
| A2 | 14 | 0.3 | 0.2 | 1.1 | 0.9 |
| A3 | 14 | 0.3 | 0.2 | 1.2 | 1.1 |
| A4 | 14 | 0.5 | 0.5 | 1.3 | 0.9 |
| A5 | 11 | 0.1 | 0.1 | 1.2 | 1.2 |
| A6a | 9 | - | - | 1.5 | 1.0 |
| A6b | 9 | - | - | 1.5 | 0.8 |
| B1 | 15 | 1.8 | 03 | 4.6 | 1.6 |
| B2 | 16 | 22.6 | 3.7 | 3.9 | 3.2 |
| B3 | 15 | 1.3 | 0.2 | 2.5 | 2.6 |
| B4 | 10 | 0.2 | 0.1 | 1.8 | 2.3 |
| B5 | 16 | 2.3 | 0.9 | 2.9 | 2.1 |
| B6 | 15 | 3.6 | 0.5 | 6.2 | 2.1 |
| B7 | 16 | 2.4 | 0.9 | 5.0 | 3.2 |
| B8 | 17 | 24.6 | 0.8 | 9.0 | 2.9 |
| B9a | 9 | - | - | 1.7 | 0.9 |
| B9b | 9 | - | - | 2.3 | 1.4 |
| B9c | 9 | - | - | 1.3 | 1.2 |
| C1 | 12 | 1.7 | 0.9 | 3.7 | 3.9 |
| C2 | 12 | 3.0 | 0.9 | 3.1 | 4.5 |

method outlined in ARI 540 is commonly used by refrigerator/freezer compressor manufacturers to generate maps of compressor performance using calorimeter data. The method uses a bivariate cubic polynomial with cross-terms to describe the mass flow rate (or capacity) and the electrical power input as a function of saturated evaporating and condensing temperatures (Equation 1).

$$X = C_1 + C_2 \cdot T_{evap} + C_3 \cdot T_{cond} + C_4 \cdot T_{evap}^2 + C_5 \cdot T_{evap} \cdot T_{cond} + C_6 \cdot T_{cond}^2 + C_7 \cdot T_{evap}^3 + C_8 \cdot T_{cond} \cdot T_{evap}^2 + C_9 \cdot T_{evap} \cdot T_{cond}^2 + C_{10} \cdot T_{cond}^3 \qquad (1)$$

where

$X$ = mass flow rate, capacity, current or power

$T_{evap}$ = saturated suction temperature

$T_{cond}$ = saturated discharge temperature

$C_1 \ldots C_{10}$ = curve fit parameters

The computer program distributed with ARI Standard 540 uses an unweighted linear least squares regression to determine the 10 parameters in Equation 1. Since Equation 1 uses ten curve fit parameters, a minimum of ten measured data points of each dependent variable at different operating conditions is necessary to estimate all the parameters.

Each of the 21 sets of mass flow rate and power data were fit to the form in Equation 1. The results are shown in Table 1. In most cases, the polynomial represented the data very well; however, Equation 1 does not incorporate any physical mechanisms of compressor operation and the resulting fits do not always make physical sense. As a result, interpolation and extrapolation based on Equation 1 can result in significant errors.

Interpolation and extrapolation inaccuracies resulting from the application of Equation 1 become more apparent when the specific power (power input divided by the mass flow rate) is plotted as a function of evaporating temperature, as shown in Figure 1. The physics governing compressor performance indicate that the specific power should consistently decrease with increasing saturated evaporating temperature and increase with increasing saturated condensing temperature. Figure 1 shows the measured data points as well as the polynomial curve fit extrapolated to higher and lower saturated evaporating and condensing temperatures for data set B5. Extrapolation appears to follow physical principles for high saturated evaporating temperatures; however, the highest and lowest saturated condensing temperature curves cross over the other curves, which is physically unrealistic. At low saturated evaporating temperatures, predictions seem very inaccurate even for condensing temperatures that were represented in the data.

One of the data sets used in this investigation contained only ten data points (B4). Since there are ten coefficients in Equation 1, these coefficients can be completely determined with ten independent tests so that the polynomials perfectly fit

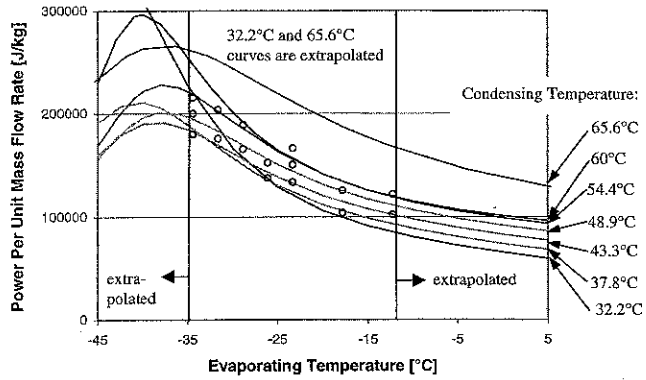


*Figure 1 Polynomial curve fit, specific power as a function of saturated evaporating temperature for a range of saturated condensing temperatures (data set B5).*

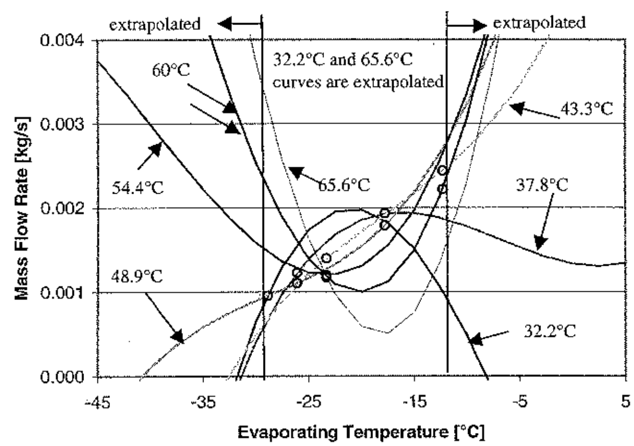


*Figure 2 Mass flow rate map determined by ARI 540 computer program (data set B4).*

the data. Figure 2 shows the resulting curves, as determined by the program provided with ARI Standard 540, for these ten data points. It is clear that the measured data points agree almost perfectly with the fits (0.2% relative error on average, which we believe is due to round-off errors resulting from single-precision calculations), but both interpolation and extrapolation do not make physical sense.

## CURVE FIT PROCEDURE

Several different models have been investigated during this research. Each model contained a number of regression parameters that are estimated by using a least squares curve fit. The objective function for the curve fit is given by Equation 2.

$$OF = \sqrt{\frac{\sum_{i=1}^{N} \left(\frac{X_{meas} - X_{calc}}{X_{mean}}\right)^2}{N}} \qquad (2)$$

where

$OF$ = objective function

$N$ = number of data points

$X_{meas}$ = measured mass flow rate or power

$X_{calc}$ = calculated mass flow rate or power

$X_{mean}$ = average of all measured mass flow rate or power data

A nonlinear regression technique is used to minimize the value of the objective function by altering the values of the parameters within specified bounds. Normalizing the error with the average of all measured values, as is done in Equation 2, ensures that all data points are weighted equally.

## MASS FLOW RATE MODEL

Mass flow rate for a compressor can be determined knowing its volume flow and the refrigerant density at the compressor suction. In general, positive displacement compressors are nearly constant volumetric flow devices; however, deviations from constant volume flow occur and can be accounted for by using a volumetric efficiency. The volumetric efficiency of a reciprocating compressor is defined as the ratio of the actual refrigerant volumetric flow rate to the displacement rate of the compressor. A number of factors contribute to reducing the volumetric efficiency of a compressor including the clearance volume and leakage around the piston (which is influenced by the compression ratio). The volumetric efficiency of a reciprocating compressor can be approximated by Equation 3 in terms of $C$, the clearance volume ratio, and $n$, polytropic compression exponent (Threlkeld 1962).

$$\eta_v = 1 - C\left[\left(\frac{P_{discharge}}{P_{suction}}\right)^{1/n} - 1\right] \tag{3}$$

with

$C$ = effective clearance volume ratio

$P_{discharge}$ = absolute discharge pressure

$P_{suction}$ = absolute suction pressure

$n$ = polytropic exponent

The refrigerant mass flow rate can then be calculated knowing the displacement rate of the compressor and the specific volume of the refrigerant at the suction side of the compressor using Equation 4.

The available experimental data provided information relating the refrigerant mass flow rate to suction and discharge pressures. These data were subjected to nonlinear regression in order to determine the values of $C$ and $n$ that produce a "best fit" to the experimental data. It was found that the values of $C$ and $n$ determined in this manner are not independent of each other. For example, the polytropic index could be set to any value and a corresponding value of $C$ could be determined by linear regression, which would be a good fit to the experimental data as if both $C$ and $n$ were independently determined. Our recommendation is to set the polytropic exponent to the ratio of the constant pressure to constant volume specific heats (evaluated for the given refrigerant at the compressor suction condition of each data point) and then find the best value for $C$.

The available data express the compressor performance for a given refrigerant as a function of the saturated evaporating and condensing temperatures. Knowing the thermodynamic properties of the refrigerant allows the corresponding pressures to be determined. However, the refrigerant undergoes a pressure drop as it passes into or out of the compressor shell and through the valves of the compressor. The pressure drop on the high-pressure side of the compressor was found to have little effect on the refrigerant mass flow rate or the compressor power; however, the pressure drop on the low-pressure side, although small, can have a significant effect on the refrigerant mass flow rate. A suction pressure drop term has been introduced into the mass flow rate model to capture this effect. This pressure drop term, $\delta P$, is presented as a constant percentage of the evaporating pressure. Equation 4 shows the final model. It has two parameters, $C$ and $\delta p$. These parameters have some physical meaning, but they should be regarded as curve fit parameters because they account for phenomena that occur in the compressor but are not directly represented in the model.

$$\dot{m}_{calc} = \left\{1 - C\left[\left(\frac{p_{cond}}{p_{evap}(1-\delta p)}\right)^{1/k} - 1\right]\right\} \cdot \frac{V \cdot RPM}{v_{suction} \cdot 60} \tag{4}$$

where $k$ is the specific heat ratio.

Internal heat transfer is one more important physical process that impacts the volumetric efficiency of a small hermetic compressor. Heat transferred from the hot zones of the compressor (e.g., the motor windings and discharge manifold in the cylinder head) to the suction gas raises the temperature of the suction gas, lowering the density, and, therefore, lowers the volumetric efficiency by changing the inlet conditions to the compressor shell. While the model formulation in Equation 4 does not address these phenomena explicitly, the effect of heat transfer on the volumetric efficiency is similar to the effect on the volumetric efficiency of the suction pressure losses represented by the $\delta p$ term. Since $\delta p$ is determined by curve fit, it tends to capture the combined effect on the measured data of both suction pressure losses and the thermodynamic loss due to internal heat transfer to the suction gas.

Figure 3 and Table 2 compare the mass flow rate model to the experimental data points for one set of data. The average relative error is only 1.3% with a maximum error of 1.7%. Similar results are obtained from most of the 20 sets of data that were used in this study (see Table 1). The errors for data sets B1 through B8 are much bigger than for the other data sets. The ten-parameter polynomials also fit less well for these data sets. This seems to indicate that these data sets include inaccurate data points. For some data sets, these inaccuracies become obvious when the data are plotted in form of a compressor map. The mass flow rate map of Figure 3 has been extrapolated to higher and lower condensing and evaporating

**TABLE 2**
**Relative Errors for Mass Flow Rate Model for Data Set A4**

| $T_{evap}$ (°C) | $T_{cond}$ (°C) | Relative Error |
|---|---|---|
| -12.2 | 37.8 | -1.4% |
| -17.8 | 37.8 | 1.6% |
| -23.3 | 37.8 | 1.5% |
| -28.9 | 37.8 | 1.6% |
| -23.3 | 40.6 | 1.1% |
| -12.2 | 43.3 | -1.0% |
| -17.8 | 43.3 | 1.5% |
| -23.3 | 43.3 | 1.4% |
| -28.9 | 43.3 | -1.4% |
| -12.2 | 48.9 | -0.1% |
| -17.8 | 48.9 | 0.9% |
| -23.3 | 48.9 | -1.6% |
| -28.9 | 48.9 | -1.1% |
| -23.3 | 54.4 | -1.7% |
| | Average | 1.3% |

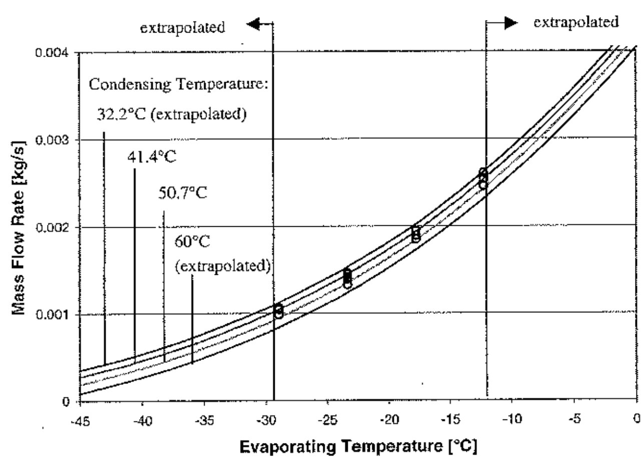


***Figure 3*** *Extrapolated mass flow rate map (data set A4).*

temperatures than represented in the experimental data, as discussed further in the "Extrapolation Capabilities" section of this paper.

## POWER MODEL

Electrical power is supplied to the electric motor in the hermetic shell. The motor efficiency is less than unity, so some of the electrical power is dissipated as heat. Some of this heat is convected to the low-pressure refrigerant entering the hermetic compressor shell, thereby raising the temperature of the inlet refrigerant and lowering the compressor's volumetric efficiency. The electrical power input to the compressor has been modeled based on estimating the work necessary for a polytropic compression process as well as an efficiency term that includes the electric motor efficiency and other inefficiencies that occur inside a compressor, such as frictional effects. Equation 5 shows the power model including this combined efficiency, $\eta_{comb}$.

$$Power \cdot \eta_{comb} = \dot{m} \cdot \frac{k}{k-1} \cdot p_{suction} \cdot v_{suction}\left[\left(\frac{P_{discharge}}{P_{suction}}\right)^{\frac{k-1}{k}} - 1\right] \tag{5}$$

where $p_{suction} = (1 - \delta_p)p_{evap}$ and $p_{discharge} = p_{cond}$.

The same suction and discharge conditions were used as for the mass flow rate model, i.e., the discharge pressure is set to the pressure in the condenser and the suction pressure is estimated using $\delta p$, the pressure drop parameter defined for the mass flow rate model. The polytropic exponent, $n$, is set to the specific heat ratio, $k$, at the compressor inlet condition, as in the refrigerant mass flow rate model. We have found that using the mass flow rate calculated with the model rather than the experimental mass flow rate tends to smooth out the mass flow rate data and provide a slightly better fit for the power.

Only one unknown parameter remains in Equation 5—the combined efficiency, $\eta_{comb}$. The combined efficiency was found not to be a constant. In order to identify a functional relation for the combined efficiency, values of the combined efficiency that perfectly fit the data for each point in the data set were plotted against pressure ratio and evaporating and condensing temperature. The data scatter least when plotted against the evaporating pressure. Several relationships were considered to represent the variation of the combined efficiency with operating conditions. Equation 6 shows the exponential equation that provided the best fit to the data.

$$\eta_{comb} = d + e \cdot \exp(f \cdot p_{evap}) \tag{6}$$

where $d$, $e$, and $f$ are regression parameters.

Figure 4 shows a map for power generated with this model (Equations 5 and 6, data set A4). The experimental data included saturated evaporator temperatures ranging from –28.9°C (–20°F) to 12.2°C (10°F) and saturated condensing temperatures from 37.8°C (100°F) to 54.4°C (130°F). The figure illustrates model agreement in the range for which experimental data were available as well as extrapolation to saturated evaporator and condenser temperatures outside of the measured data range. Table 3 shows the relative error for each data point as well as the average relative error for all points for data set A4. See Table 1 for results of all data sets.

The specific power has been plotted for data set A4 as a function of evaporating temperature in Figure 5. The map of the specific power (shown in Figure 5) appears to be reasonable. The specific power increases consistently with decreasing evaporating temperature and with increasing condensing temperature, and the lines representing a fixed condensing

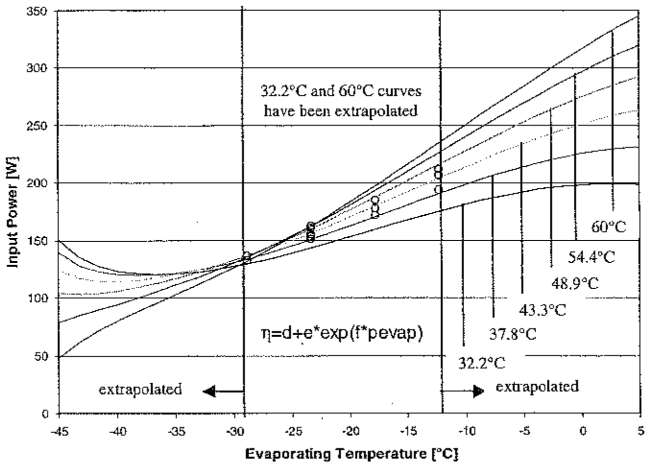


*Figure 4* *Extrapolated power map using the exponential relationship for the combined efficiency (data set A4).*

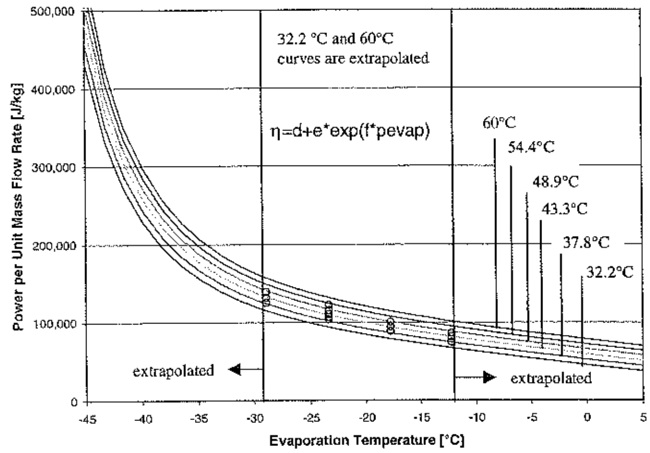


*Figure 5* *Extrapolated power per unit mass flow rate map for the combined efficiency (data set A4).*

**TABLE 3**
**Errors for the Exponential Power Model (Data Set A4)**

| $T_{evap}$ (°C) | $T_{cond}$ (°C) | Relative Error |
|---|---|---|
| -12.2 | 37.8 | -1.7% |
| -17.8 | 37.8 | -0.8% |
| -23.3 | 37.8 | -0.5% |
| -28.9 | 37.8 | 0.8% |
| -23.3 | 40.6 | -0.1% |
| -12.2 | 43.3 | -1.1% |
| -17.8 | 43.3 | 0.8% |
| -23.3 | 43.3 | 0.4% |
| -28.9 | 43.3 | -0.6% |
| -12.2 | 48.9 | 2.0% |
| -17.8 | 48.9 | 1.1% |
| -23.3 | 48.9 | -0.5% |
| -28.9 | 48.9 | 0.1% |
| -23.3 | 54.4 | -0.1% |
| | Average | 0.9% |

**TABLE 4**
**Relative Errors for Extrapolation to Higher Condensing and Higher Evaporating Temperatures (Data Set A4)**

| | Operating Conditions | | Relative Errors | |
|---|---|---|---|---|
| | Condensing Temperature (°C) | Evaporating Temperature (°C) | Mass Flow Rate | Power |
| Used for model parameter fitting | 37.8 | -23.3 | -0.1% | -0.4% |
| | 37.8 | -28.9 | 1.3% | 0.2% |
| | 40.6 | -23.3 | -0.2% | 0.4% |
| | 43.3 | -28.9 | -0.8% | -0.2% |
| | Average: | | 0.8% | 0.3% |
| Not used for model parameter fitting | 37.8 | -12.2 | -4.5% | -2.8% |
| | 37.8 | -17.8 | -0.9% | -1.2% |
| | 43.3 | -12.2 | -3.6% | -2.0% |
| | 43.3 | -17.8 | -0.5% | 0.7% |
| | 48.9 | -12.2 | -2.3% | 1.4% |
| | 43.3 | -23.3 | 0.5% | 1.1% |
| | 48.9 | -17.8 | -0.4% | 1.5% |
| | 48.9 | -23.3 | -1.7% | 0.9% |
| | 48.9 | -28.9 | 0.9% | 1.7% |
| | 54.4 | -23.3 | -0.8% | 2.2% |
| | Average: | | 2.1% | 1.7% |

temperature do not cross. Additional validity checks of the extrapolation capabilities of the model are described in the following section.

## EXTRAPOLATION CAPABILITIES

A method for representing calorimeter test data has been proposed that requires only two curve fit parameters in the mass flow rate equation (Equation 4) and three parameters for the power equation (Equations 5 and 6). In theory, three measurements of mass flow rate and power at three different conditions are sufficient to determine the five parameters involved in this representation. In contrast, 20 parameters are needed if mass flow rate and power were represented with polynomials of the form shown in Equation 1.

To test the extrapolation capabilities of the proposed models, the five parameters were determined using different combinations of four or five measured data points. The estimated parameters were then used in Equations 4 through 6 to predict mass flow rate and power at independent operating conditions for which measured data were available. Then predicted and measured data were compared.

For example, four data points at low evaporating and low condensing temperatures were selected from the test data and the five parameters were fit using these measurements. Table 4 shows these data points as well as the other ten independent data points extrapolated using the model.

Extrapolation was tested for saturated condensing and evaporating temperatures up to 10°C (18°F) from the data that were used to do the curve fit. The relative error for extrapolation was less than 10% for all data, and for most data points it was well under 5%. Of course, extrapolation becomes less reliable as deviations from the measured data increase.

Interpolation was tested by using the four most extreme operating conditions to determine the curve fit parameters. Relative errors for the extrapolated data points are below 3% for all data points.

To achieve acceptable extrapolation capabilities, we found it necessary to use at least four data points representing two different evaporating and two different condensing temperatures as a basis for estimating model parameters. We recommend using the four most extreme operating conditions in which the compressor is expected to operate to minimize the need for extrapolation. A fifth measurement should be taken at an intermediate operating condition to verify the curve fit.

## EFFECT OF AMBIENT TEMPERATURE

Standard calorimeter tests for domestic refrigerator/freezer units are performed at an ambient temperature of 32°C (90°F). In these tests, the compressor suction temperature and the liquid line temperature are set equal to the ambient temperature. In normal operation, however, the compressor may operate at ambient conditions well below 32°C (90°F). The temperature of the refrigerant exiting the evaporator may be considerably below 32°C (90°F) as controlled during calorimeter tests. The model, presented in Equations 4 through 6, does not have the ability to separately consider the effects of ambient and suction temperatures. In the following results, these two temperatures are assumed to be equal. Although not completely accurate, this assumption is reasonable because the liquid temperature approaches the ambient temperature in the condenser and the suction temperature approaches the liquid temperature in the interchanger. A higher suction temperature causes the specific volume at the inlet of the compressor to be larger and the mass flow rate of refrigerant to be smaller. There is little reduction in power because the specific work increase is countered with a reduction in refrigerant flow rate. The ambient temperature also affects the amount of heat transfer from the shell to the surroundings. The second effect is not taken into account by the model.

The change in mass flow rate and power that the model predicts for different ambient temperatures has been compared with the very little data available in the literature (Haider et al. 1997; Bullard 1998) and with experimental data from one compressor manufacturer. It was found that the model's predictions are reasonably accurate as shown in Table 5. Relative errors are less than 2%, except for measurements at 15.6°C (60°F). At this very low ambient temperature, the condensing temperatures were much lower than the ones used to fit the model parameters. The inaccuracies of extrapolating to 22°C (40°F) lower condensing temperature and to 16.7°C (30°F) lower ambient temperature are confounded in this case, and relative errors for power range from 8% to 12%.

## CONCLUSIONS

Bicubic polynomials are commonly used to generate maps that represent calorimeter measurements of refrigerant mass flow rate and power for the small hermetic compressors employed in refrigerator/freezer appliances. These polynomials may fit the experimental data well, but they do not allow reliable extrapolation or interpolation of the data. In addition, more than ten measurements of mass flow rate and power are necessary for this method.

A semi-empirical method has been investigated to represent the performance of reciprocating refrigerator/freezer compressors. The model can be used to estimate the refrigerant mass flow rate and power using as few as four experimental data points. The model interpolates and extrapolates reliably up to 10°C (18°F) higher and lower evaporating and condensing temperature. Relative errors in mass flow rate and power are below 5%.

The effect of ambient temperature seems to be well represented in the model as a change in specific volume of the refrigerant at the suction side of the compressor. No data were available to test the model for the case in which the ambient and suction temperatures are not close to each other.

All the data used in this research were taken using forced air cooling over the compressor shell. The model does not extrapolate from static (zero air velocity) cooling to forced cooling or vice-versa.

## RECOMMENDATIONS

To minimize the need to extrapolate, it would be useful to take four measurements at the extreme points of the range of operating conditions in which the compressor is expected to work to fit the five model parameters. A fifth measurement should be taken at intermediate operating conditions that can be used to verify the model (Figure 6). If a single point is to be used to represent compressor performance, we recommend that the conditions should be 40.6°C (105°F) saturated condensing and –23.3°C (–10°F) saturated evaporating temperature at 32.2°C (90°F) compressor suction, liquid line, and ambient temperature. This condensing temperature more closely represents the conditions at which the forced air condensers in modern refrigerator/freezers operate. This single rating point should also be used as the center point of the five recommended measurements as shown in Figure 6. The accuracy and method of testing should be in accordance with *ASHRAE Standard 23-1993* (ASHRAE 1993).

**TABLE 5**
**Predictions at Different Ambient Temperatures**
**(Measured Data from Haider et al. [1997], Compressor D)**

| Ambient Temperature (°C) | $T_{cond}$ (°C) | $T_{evap}$ (°C) | Mass Flow Rate meas. (kg/s) | Mass Flow Rate calc. (kg/s) | Mass Flow Rate Relative Error | Power meas. (kg/s) | Power calc. (kg/s) | Power Relative Error |
|---|---|---|---|---|---|---|---|---|
| 32.2 | 54.4 | -28.9 | 0.001148 | 0.001138 | -0.9% | 118.3 | 118.2 | -0.1% |
| | 48.9 | -28.9 | 0.001184 | 0.001184 | 0.0% | 115.8 | 116.2 | 0.3% |
| | 43.3 | -28.9 | 0.001225 | 0.001225 | 0.0% | 113.6 | 113.2 | -0.4% |
| | 54.4 | -23.3 | 0.001511 | 0.001528 | 1.1% | 135.9 | 136.6 | 0.5% |
| | 48.9 | -23.3 | 0.001586 | 0.001575 | -0.7% | 132.4 | 132.3 | -0.1% |
| | 43.3 | -23.3 | 0.00162 | 0.001617 | -0.2% | 127.7 | 127.1 | -0.5% |
| | 54.4 | -17.8 | 0.00197 | 0.001994 | 1.2% | 154.4 | 155.6 | 0.8% |
| | 48.9 | -17.8 | 0.002039 | 0.002041 | 0.1% | 148.9 | 148.9 | 0.0% |
| | 43.3 | -17.8 | 0.002113 | 0.002084 | -1.4% | 142.6 | 141.2 | -1.0% |
| 43.3°C | 54.4 | -28.9 | 0.001091 | 0.001097 | 0.5% | 116.6 | 117.9 | 1.1% |
| | 48.9 | -28.9 | 0.001144 | 0.001141 | -0.3% | 114.3 | 115.9 | 1.4% |
| | 54.4 | -23.3 | 0.00149 | 0.001473 | -1.1% | 134.5 | 136.2 | 1.3% |
| | 48.9 | -23.3 | 0.001502 | 0.001518 | 1.1% | 130.4 | 132 | 1.2% |
| 15.6°C | 26.7 | -28.9 | 0.001376 | 0.001408 | 2.3% | 106.9 | 98.71 | -7.7% |
| | 23.9 | -28.9 | 0.001436 | 0.001424 | -0.8% | 104.6 | 95.46 | -8.7% |
| | 26.7 | -23.3 | 0.001846 | 0.001825 | -1.1% | 117.3 | 106.0 | -9.6% |
| | 23.9 | -23.3 | 0.001885 | 0.001841 | -2.3% | 115.1 | 101.7 | -11.6% |

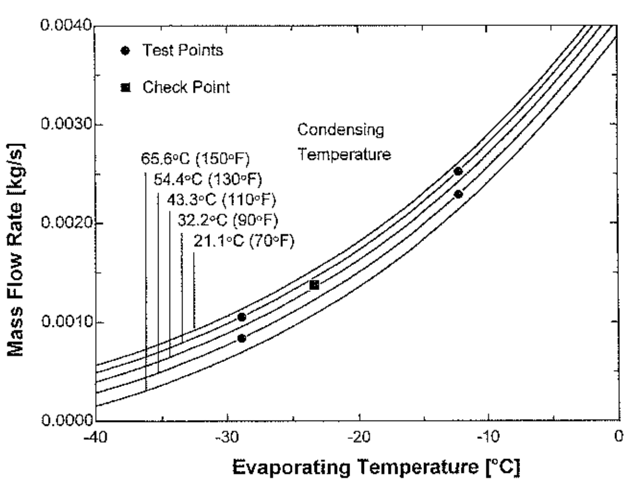


*Figure 6* *Recommendations of four test conditions.*

## ACKNOWLEDGEMENTS

The research conducted for this paper was funded by ASHRAE TC 7.1 as ASHRAE research project RP-870. The authors are grateful to the project monitoring subcommittee for their input on the project. The project monitoring subcommittee members included Clark Bullard, Tom Davis, Ed Wuesthoff, John Diekmann, John Sabelli, and Behrooz Mohebbi.

## REFERENCES


ARI. 1991. *ARI Standard 540, A method for presentation of compressor performance data.* Air-Conditioning and Refrigeration Institute.

ARI. 1999. *ARI Standard 540, A method for presentation of compressor performance data.* Air-Conditioning and Refrigeration Institute.

ASHRAE. 1993. *ASHRAE/ANSI Standard 23-1993, Methods of testing for rating positive displacement refrigerant compressors and condensing units.* Atlanta: American Society of Heating, Refrigerating and Air-Conditioning Engineers, Inc.

AHAM. 1993. *AHAM Guide to the National Appliance Conservation Act.* Washington DC: Association of Home Appliance Manufacturers. http://www.aham.org/mfrs/govt/effic/naecagd.pdf.

Bullard, C. 1998. Personal conversation, experimental data.

Haider, I., M. Lavannis, and R. Radermacher. 1997. Investigations of the EPA refrigerator analysis (ERA) software: Compressor map and ambient temperature effects. *ASHRAE Transactions* 103 (1): 608-618.

Jähnig, D. 1999. A semi-empirical method for modeling reciprocating compressors in residential refrigerators and freezers. M.S. thesis, Solar Energy Laboratory, Department of Mechanical Engineering, University of Wisconsin–Madison.

Klein, S.A., and D.T. Reindl. 1999. Develop data base for determining optimum compressor rating points for residential refrigerator and freezer compressors, Final report, ASHRAE Research Project RP-870.

Threlkeld, J.L. 1962. *Thermal environmental engineering*. Englewood Cliffs, NJ: Prentice-Hall.